Digital Object Identifier (DOI): 10.1109/CPE.2017.7915153

2017 11th IEEE International Conference on Compatibility, Power Electronics and Power Engineering (CPE-POWERENG), Cadiz, 2017, pp. 106-111.

Waveform peak shaping by multi-frequency power transfer in internal, single-phase distribution systems

Sebastian Brüske
Giampaolo Buticchi
Marco Liserre

Waveform Peak Shaping by Multi-Frequency Power Transfer in Internal, Single-Phase Distribution Systems

Sebastian Brüske, Giampaolo Buticchi and Marco Liserre
Christian-Albrechts-Universität zu Kiel
Kaiserstr. 2, 24143 Kiel, Germany
Email: seb@tf.uni-kiel.de

***Abstract*—Internal distribution systems such as photovoltaic parks allow to use DC or AC with a frequency different from 50Hz. In this paper is instead proposed to use more than one frequency at the same time. The grid voltage amplitude at the fundamental frequency can be increased while the voltage peak value is kept constant by adding odd harmonics to the voltage waveform. The currents are decreased for the same power level which leads to reduced power converter losses. A further current reduction is achieved if waveform peak shaping is applied to the current waveforms. This paper presents the impact of multi-frequency power transfer on single-phase converters, and verifies the results with analysis and simulations. The impact of harmonic frequencies on cable losses due to the skin effect is taken into consideration in the analysis and effects on protection are discussed.**

Keywords*—pulse-width modulated power converters, multi-frequency power transfer, internal distribution.

I. Introduction

The renewable energy exploitation and power electronics development have been proceeding at the same rate, and power electronics converters have been widely adopted to feed power into the electric grid [1], or to power isolated systems. When integrating multiple energy sources, or multiple photovoltaic (PV) panels, it is a very desirable characteristic to harvest the maximum possible power. Centralized systems, with a single converter rated for the full power and multiple PV strings connected in parallel do not allow the independent tracking of the maximum power, because of the difference between strings and single panels, or because of partial shading. This is why multi-stage concepts with a common bus gained popularity [2]. The common bus constitutes a local distribution system, that can be interfaced to the grid (low-voltage (LV) or medium-voltage (MV)) via a conventional transformer, or a centralized power converter, or it can represent an isolated micro-grid [3].

The common bus can be either in AC or in DC. While DC distribution would be beneficial due to the reduction of conversion stages, high-voltage DC (400V-700V) is encountering serious difficulties due to the cost of breakers and for safety reasons. Since LV DC distribution would imply unacceptable costs in terms of cabling and would require high step-up conversion stages, AC distribution for the local bus is often preferred. Isolated or internal AC distribution allows to use grid frequencies different from 50/60Hz (e.g. 400Hz in aircraft) for optimization of the grid components, such as reduced transformer sizes.

This paper refers to this framework: an independent, internal AC distribution with multiple grid-connected converters. In these conditions, the basic constraint of having a sinusoidal voltage waveform cease to exist, and new possibilities regarding the optimization of the AC bus arise. Power electronics converters are able to generate arbitrary voltage waveforms at their output terminals, which can vary from simply square wave to pulse-width modulated signals. Simultaneous power transfer at different frequencies has been recently applied to power electronics, described in [4] in general terms. By forming nested secondary power loops that are independent of the main power loop, control tasks such as capacitor voltage balancing can be implemented. A 3rd harmonic injection approach in transmission systems to lower the conductor-to-ground clearance is proposed in [5]. In systems based on inductive power transfer a decoupled power transfer of mutually coupled receivers can be realized, or the power transfer in single-receiver systems can be optimized with regard to decrease the field emissions by reducing the peak value of the produced fields [6].

This paper explores the possibility of implementing voltage and current waveform peak shaping for grid-connected power electronics converters in distribution systems. By superposition of odd harmonics the peak value of a sinusoidal waveform can be reduced and the amplitude of the fundamental component can be increased in respect to the initial value without exceeding the maximum voltage rating. This principle is a well-known approach to optimize the DC-link voltage utilization in three-phase power converters. It is used in [5] to lower the voltage without changing the fundamental component. Applied to single-phase distribution systems, new optimization possibilities arise, which are presented in this paper. For a given power level the corresponding current at the fundamental frequency is decreased if waveform peak shaping is applied to the voltage waveform resulting in reduced power converter losses. A further reduction can be achieved with current waveform peak shaping. DC-link power oscillations can be reduced, and higher power converter and grid efficiencies are reached.

The paper is organized into four sections. The idea and motivation of waveform peak shaping and a possible implementation in a single-phase PV and μWind distribution plant based on a central power converter are discussed in Section II. The impact on single-phase power converters in terms of control and instantaneous power behavior in a dual-

frequency system is described in Section III and the frequency dependency of the line parameters are discussed. The power converter efficiency and the impact on the grid efficiency are evaluated by simulations in Section IV. Conclusions are finally drawn in Section V.

II. Waveform Peak Shaping in Internal Distribution

In this section the idea of waveform peak shaping in a distribution plant is explained and a possible grid scenario in which it can be implemented is described.

A. Peak Shaping of a Sinusoidal Waveform

The components in the distribution plant are rated for a nominal voltage and current amplitude that can be seen as the main design factors of power electronics converters. The shape of sinusoidal waveforms can be influenced by superposition of multiple frequency components. For example, the 3rd harmonic injection PWM is a well-known approach in three-phase voltage source inverters to increase the maximum modulation index [7]. The injection of odd harmonics cuts the peak of the fundamental component and it allows increasing the amplitude of the fundamental frequency without exceeding the initial peak value of the waveform. The RMS value of the signal is increased without changing the total peak value. The maximum increase of the fundamental amplitude is achieved by a square wave signal:

$$x(t) = \frac{4X_0}{\pi} \sum_{k=1}^{\infty} \frac{\sin((2k-1)\omega_1 t)}{2k-1} \tag{1}$$

where ω_1 denotes the base frequency and X_0 is the peak value of the signal. It means that the fundamental amplitude can be increased by 27.3% in comparison to the pure sinusoidal waveform. Due to the infinite number of frequency components it is a theoretical maximum that can not be reached in practice. In this work, a dual-frequency system is analyzed for simplicity, but more frequency components can be added to the system. The superposition of a sinusoidal signal and the additional frequency can be described by

$$\begin{aligned} x(t) &= X_1 \sin(\omega_1 t) + X_n \sin(\omega_n t) \\ &= X_1 \sin(\omega_1 t) + x_\mathrm{r} X_1 \sin(n\omega_1 t) \end{aligned} \tag{2}$$

with n as the harmonic order of the second system frequency. The maximum increase of X_1 is reached for $x_{\mathrm{r,opt}} = 1/6$, which means an increase by 15.47% [7]. Due to this, the 3rd harmonic frequency is chosen for analysis of a dual-frequency system in this paper.

B. Single-Phase PV and μWind Distribution Plant with Central Power Converter

The concept of a single-phase, LV AC distribution system connecting several PV and μWind power plants is shown in Fig.1, in which a central power converter sets the grid voltage of an isolated distribution system. The central power converter acts as the link between the distribution system and the main grid that can be an AC grid in LV or MV or it can be a DC grid. The amplitude and frequency of the system voltage is controlled by the central power converter fixed to the reference values. The amplitude and shape of the current

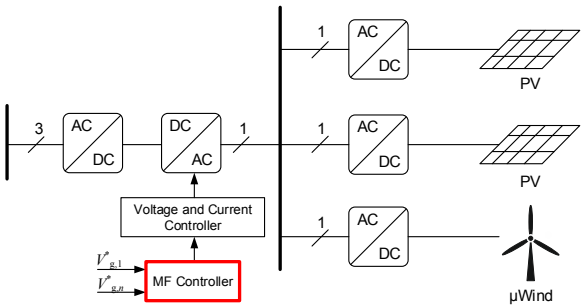

Fig. 1. PV and μWind distribution plant with single-phase inverters based on a central power converter.

waveform is determined by the control of the power plants. The voltage waveform, instead, is set by the main power converter control. The main power converter control is implemented by means of nested control loops: an inner voltage and current control loop where the AC voltage waveform is controlled, and the outer MF control loop where the voltage waveform reference is imposed (red box). In a dual-frequency system and implemented waveform peak shaping, the voltage reference consists of two superimposed signals: the $50\,\mathrm{Hz}$ sinusoidal voltage reference, typical of electrical grid applications, and the sinusoidal waveform at an odd harmonic frequency.

III. Single-Phase Inverters in a Dual-Frequency System

An overview of the control concept of a dual-frequency, single-phase inverter is given in Fig.2, where an inverter is connected to a power system by an LC-filter. The system voltage consists of two frequency components: The fundamental and the odd harmonic frequency. The inverter grid-side control consists of a grid synchronization for both frequencies and a double-loop control scheme. The outer power controller sets the current references for the inner current control loop in dependence on the active power reference. The current controller generates the according inverter output voltage from which the gate signals are calculated by pulse-width modulation (PWM). A more detailed description of MF inverter control is given in [8], [9] for a point-to-point power transfer at an additional frequency in a distribution system. In the following, the instantaneous power of a single-phase inverter in a dual-frequency system is analyzed. Moreover, the main effects of additional frequencies on power cable parameters and effects on protection are discussed.

A. Instantaneous Power of Single-Phase Inverters

If the high frequency components introduced by the PWM are neglected, the inverter voltage and current are represented by the fundamental and 3rd harmonic frequency components:

$$v'(t) = V_1' \sin(\omega_1 t) + V_3' \sin(\omega_3 t + \theta_3') \tag{3}$$

$$i'(t) = I_1' \sin(\omega_1 t + \varphi_{i,1}') + I_3' \sin(\omega_3 t + \theta_3' + \varphi_{i,3}') \tag{4}$$

where V' and I' are the inverter voltage and current amplitudes, θ' and φ_i' denote the phase voltage and phase current of

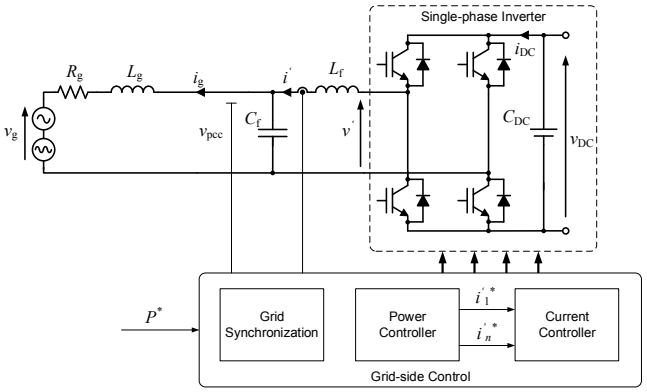

Fig. 2. Single-phase inverter in a dual-frequency system.

the inverter, respectively. From (3) and (4) the instantaneous active power is calculated as follows:

$$\begin{aligned} p'(t) &= v'(t)\cdot i'(t) \\ &= \frac{1}{2}\Big(V_1' I_1' \left[\cos(\varphi_{i,1}') - \cos(2\omega_1 t + \varphi_{i,1}')\right] \\ &\quad + V_1' I_3' \left[\cos((\omega_1-\omega_3)t - \theta_3' - \varphi_{i,3}') - \cos((\omega_1+\omega_3)t + \theta_3' + \varphi_{i,3}')\right] \\ &\quad + V_3' I_1' \left[\cos((\omega_3-\omega_1)t + \theta_3' - \varphi_{i,1}') - \cos((\omega_3+\omega_1)t + \theta_3' + \varphi_{i,1}')\right] \\ &\quad + V_3' I_3' \left[\cos(\varphi_{i,3}') - \cos(2\omega_3 t + 2\theta_3' + \varphi_{i,3}')\right] \Big) \end{aligned} \tag{5}$$

It can be noted that each frequency leads to a constant power component independent of the other frequency [4]. For waveform peak shaping only active power is considered: $\varphi_{i,1}' = \varphi_{i,3}' = 0$. With $\theta_3' = 0$ and with $\omega_3 = 3\omega_1$ the instantaneous active power results to be

$$\begin{aligned} p'(t) = &\frac{1}{2}\Big(V_1' I_1' + V_3' I_3' \\ &+ [V_1' I_3' + V_3' I_1' - V_1' I_1'] \cos(2\omega_1 t) \\ &- [V_1' I_3' + V_3' I_1'] \cos(4\omega_1 t) - V_3' I_3' \cos(6\omega_1 t) \Big) \end{aligned} \tag{6}$$

In comparison to single-phase systems with one frequency the 2nd order harmonic power oscillation is reduced by a term that generates an oscillation at the 4th harmonic frequency. In addition, power oscillations at the 6th harmonic is introduced. The inverter voltage and the instantaneous active power are shown in Fig.3 for different voltage ratios $v_r' = V_3'/V_1'$ and current ratios $i_r' = I_3'/I_1'$. The voltage peak value is set to $V_0' = 325\text{V}$ and the current amplitudes are calculated for an active power injection of $P' = 2\text{kW}$. The peak value of the power oscillations can be reduced and the choice of $x_{r,opt}$ for both v_r' and i_r' results in the highest reduction. Moreover, the shifting of the power oscillations to higher frequencies can be beneficial in terms of DC-link power losses and lifetime of the capacitors since the equivalent series resistance of electrolytic capacitors is decreasing over the frequency [10].

B. Frequency Effects on Line Parameters

The implementation of additional power frequencies higher than the fundamental frequency lead to additional cable losses due to skin and proximity effects and dielectric losses [11]. In this paper only the skin effect as the main phenomena is

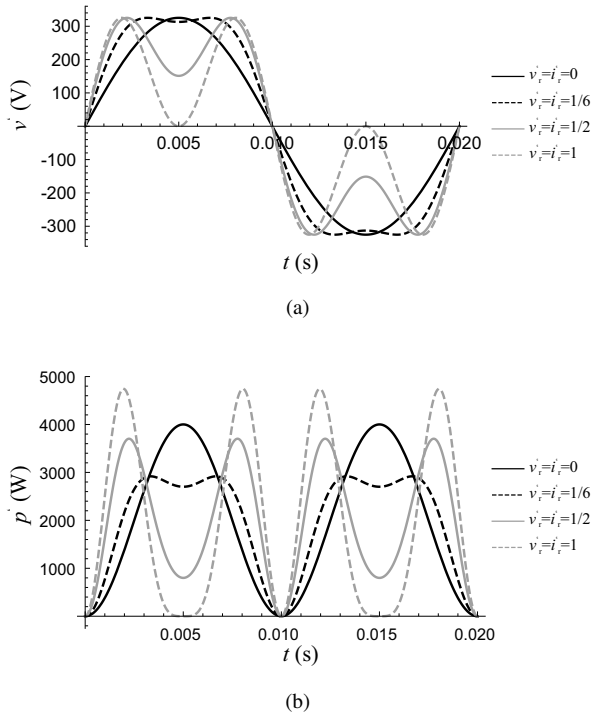

Fig. 3. Voltage waveform and resulting instantaneous active power for different voltage and current ratios (constant active power).

considered. The impact of the skin effect on the line resistance R and inductance L of a simple radial conductor with the diameter d can be approximated as described in [12]:
For $x < 1$

$$\frac{R}{R_{\text{DC}}} = 1 + \frac{x^4}{3} \tag{7}$$

$$\frac{\omega L}{R_{\text{DC}}} = x^2 \cdot \left(1 - \frac{x^4}{6}\right) . \tag{8}$$

For $x > 1$

$$\frac{R}{R_{\text{DC}}} = x + \frac{1}{4} + \frac{3}{64x} \tag{9}$$

$$\frac{\omega L}{R_{\text{DC}}} = x - \frac{3}{64x} + \frac{3}{128x^2} \tag{10}$$

with

$$x = \frac{d}{4}\sqrt{\pi\kappa\mu f} = \frac{d}{4\delta} \tag{11}$$

$$\delta = \frac{1}{\sqrt{\pi\kappa\mu f}} , \tag{12}$$

where δ is the skin depth, κ the electrical conductivity and $\mu = \mu_0\mu_r$ the permeability constant of the conductor material. The DC resistance R_{DC} can be calculated by

$$R_{\text{DC}} = \frac{1}{\pi\kappa\frac{d^2}{4}} . \tag{13}$$

In order to show the frequency dependency of the parameters R and L equations (7)-(10) are calculated for copper conductors with different cross-section at an ambient temperature of 20°C ($\kappa_{\text{Cu}} = 35.38\,\text{Sm/mm}^2$, $\mu_{\text{Cu}} = 1.256629 \cdot 10^{-6}\text{H/m}$). The results are shown in Fig. 4. Quantities ΔR and ΔL are the

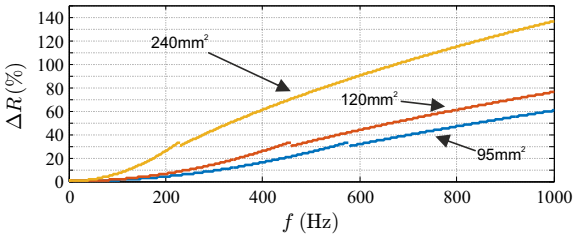

(a)

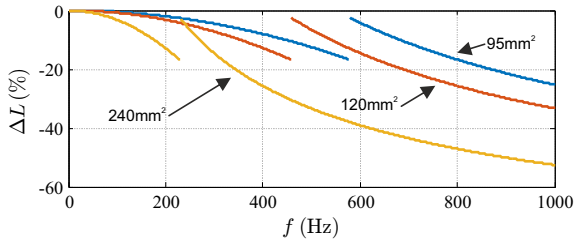

(b)

Fig. 4. Line parameter variations due to skin effect.

difference between the value at the specific frequency and the value at the fundamental frequency 50Hz. It can be seen that the frequency dependency increases with the cross-section of the conductor. For cross-sections below $120\mathrm{mm}^2$ the variation of R and L at 150Hz is below 10%, which is why the skin effect is neglected in this paper. However, for higher frequencies and for higher cross-sections the skin effect has to be considered in the loss evaluation and for the system design.

C. Impact on Protection

The operation of circuit breakers and fuses can be influenced by current harmonics [13] since fuses and thermal magnetic circuit breakers are temperature dependent and current harmonics can lead to a reduced trip point due to the additional skin effect. Moreover, an increased di/dt at zero crossings and the current sensing ability of thermal magnetic breakers can impact the protection. Whereas in 400Hz systems, such as ships and aircraft, circuit breakers and fuses with different temperature characteristics are used, significant power is not transferred at the harmonic frequencies in case of waveform peak shaping. The main power is transferred at fundamental frequency and the RMS of inverter and grid currents are reduced due to the increased fundamental voltage amplitude. The di/dt at zero crossings is increased mainly if waveform peak shaping is applied for the currents and it has to be guaranteed that the protection can operate in this condition.

Voltage harmonics can affect the operation of relays and algorithms that are based on sampled data or zero crossings [13]. Whereas zero crossings of the grid voltage are not modified in the waveform peak shaping approach, the operation of relays has to be tested under these conditions.

TABLE I. SIMULATION DATA

$V_{0,\mathrm{g}}$	325V
l_{g}	$255\mu\mathrm{H/km}$
r_{g}	$0.21\Omega\mathrm{/km}$
l_{line}	1km
L_{f}	5.2mH
C_{f}	$6.8\mu\mathrm{F}$
R_{f}	2Ω
V_{DC}	400V

IV. SIMULATION RESULTS

The impact of waveform peak shaping in a dual-frequency system on the inverter and grid losses based on the grid model shown in Fig.2 are evaluated by simulations using MATLAB Simulink and PLECS. The simulation data is given in Table I. The DC side of the inverter is connected to an ideal voltage source. The conduction and switching losses of the inverter are calculated based on the thermal description of the power semiconductors given by datasheets. The data of a four-pack module *Infineon F4-50R06W1E3* (full bridge) for single-phase applications is chosen.

A. Impact on Inverter Efficiency

In order to evaluate the inverter efficiency in dependence on the voltage and current amplitude ratios v_{r}' and i_{r}' without other influences, a simplified model with only an ideal current source connected to the inverter AC terminals is used. In this way, the inverter current and PWM modulated voltage can be set according to (3) and (4) for a constant power level. As described in Section III only active power and zero phase displacement between both voltage frequencies are considered for waveform peak shaping. The peak value V_0' of the inverter voltage is set to 110% of the grid voltage to obtain a scenario in which the inverter is feeding power into a grid. The inverter efficiency is calculated for different combinations of v_{r} and i_{r}, which is shown in Fig.5. The RMS of the inverter voltage in dependence of v_{r} is depicted in Fig.6. The initial temperature of the module is set to $100^{\circ}\mathrm{C}$. It can be seen that the efficiency of the inverter is changing with v_{r} and i_{r} in comparison to the point of operation with pure sinusoidal waveforms at the fundamental frequency, denoted as the base efficiency. The maximum efficiency is achieved at the highest voltage RMS value at $x_{\mathrm{r,opt}}$ (resulting in the lowest inverter current) and pure sinusoidal current. The efficiency is increased by 0.19% (absolute) in respect to the base value. If waveform peak shaping is additionally applied to the current waveform in this point, the efficiency is with 98.86% nearly as high as the maximum. In principle, for $v_{\mathrm{r}} < x_{\mathrm{r,opt}}$ the efficiency decreases with increasing i_{r} and for $v_{\mathrm{r}} > x_{\mathrm{r,opt}}$ it behaves the other way round. With $v_{\mathrm{r}} = x_{\mathrm{r,opt}}$ the inverter efficiency remains stable over i_{r} offering a wide range of operation for different levels of harmonic current injection.

B. Impact on Conductor Losses

It is easy to understand that for a given power level, the currents in a distribution system can reduced by voltage waveform peak shaping. However, the RMS of the currents can be further reduced by current waveform peak shaping. In order to show the effect, the RMS of the grid current i_{g} and

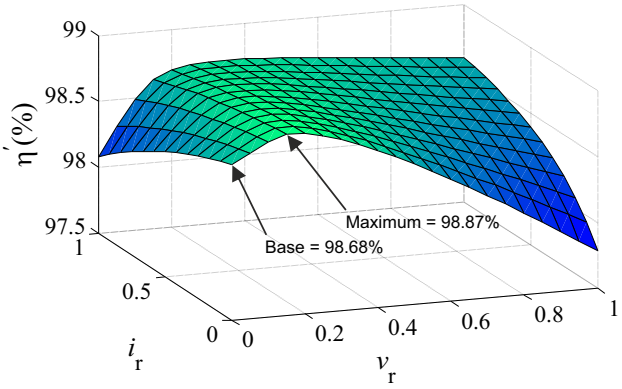

Fig. 5. Simplified grid model: Inverter efficiency for $P' = 6\text{kW}$, $V_0' = 1.1 \cdot 325\text{V}$.

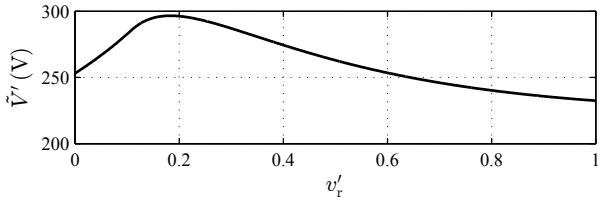

Fig. 6. Simplified grid model: RMS of the inverter voltage.

the total efficiency of the grid model consisting of the inverter, grid filter, grid impedance, and grid voltage are calculated. The conditions are the same as for the inverter efficiency evaluation with voltage waveform peak shaping applied to the grid voltage and $v_\text{r} = V_{\text{g},3}/V_{\text{g},1}$. For distribution, power cables with 120mm^2 are considered with a cable length of 1km such that the skin effect can be neglected. The results are plotted in Fig.7 and Fig. 8, respectively. The minimum RMS current is achieved, if waveform peak shaping with ratio $x_{\text{r,opt}}$ is applied to both voltage and current waveforms. The curve of the total efficiency takes a similar shape to the inverter efficiencies in Fig. 5, but the maximum efficiency is now at the point $v_{\text{r,opt}}$ and $i_{\text{r,opt}}$. The maximum is 0.77% higher than the base efficiency. This behavior can be explained by the minimization of the RMS currents, by which losses in the grid are reduced. Of course, the loss reduction is lower if frequency effects become significant depending on the system parameters.

V. Conclusion

This paper has investigated the possibility to increase the fundamental voltage amplitude in internal low-voltage distribution systems without exceeding the rated voltage by waveform peak shaping based on multi-frequency power transfer. The superposition of fundamental and odd harmonics allows to reducing the peak value of the resulting waveform in respect to the pure sinusoidal waveform. A dual-frequency system with 3rd harmonic frequency as additional frequency is chosen for analysis. The impact on power oscillations of single-phase inverters is described, indicating a reduced peak value and a shift to higher harmonics. The frequency dependency of the line parameters due to skin effect is insignificant for low-order

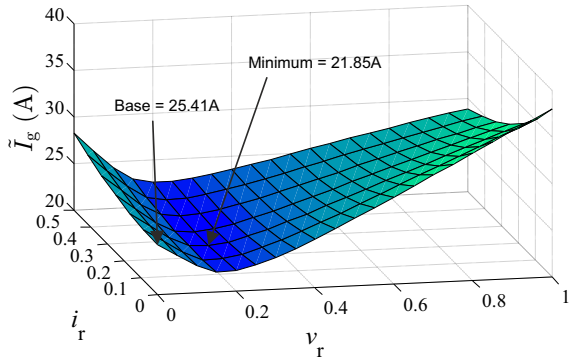

Fig. 7. RMS of grid current (neglected skin effect): $P' = 6\text{kW}$.

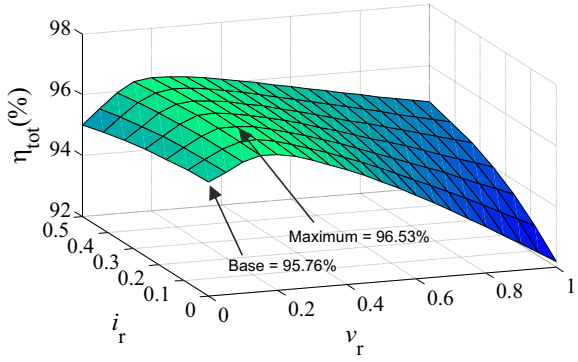

Fig. 8. Total efficiency of inverter and grid (neglected skin effect): $P' = 6\text{kW}$.

harmonics and conductor cross-sections below 120mm^2. The evaluation of the inverter semiconductor losses by simulations show that the inverter efficiency is increased by 0.19%, if voltage waveform peak shaping is applied due to reduced converter currents. It is shown that the RMS of the grid current can be minimized by current waveform peak shaping leading to reduced grid losses and an increased system efficiency by 0.77% in total without changing hardware components. The inverter efficiency and the total system efficiency remain stable at the point of optimal voltage waveform peak shaping for different levels of harmonic current injection offering a wide range of harmonic current injection.

Acknowledgment

The research leading to these results has received fundings from the European Research Council under the European Unions Seventh Framework Programme (FP/2007-2013) / ERC Grant Agreement n. [616344] and from the European Union/Interreg V-A - Germany-Denmark, under the PE:Region Project.

References

[1] B. K. Bose, "Global energy scenario and impact of power electronics in 21st century," *IEEE Trans. Ind. Electron.*, vol. 60, no. 7, pp. 2638–2651, July 2013.

[2] S. Kouro, J. I. Leon, D. Vinnikov, and L. G. Franquelo, "Grid-connected photovoltaic systems: An overview of recent research and emerging PV converter technology," *IEEE Industrial Electronics Magazine*, vol. 9, no. 1, pp. 47–61, March 2015.

[3] SMA Solar Technology, "Multicluster System 12 for SUNNY ISLAND - Easy creation of powerful on- and off-grid applications," datasheet.

[4] J. Ferreira, "The multilevel modular DC converter," *IEEE Trans. Power Electron.*, vol. 28, no. 10, pp. 4460–4465, Oct. 2013.

[5] R. Alaei and S. A. Khajehoddin, "The operation of a power transmission line with injected third harmonic voltage," *IEEE Trans. Power Del.*, vol. 32, no. 1, pp. 226–233, Feb 2017.

[6] Z. Pantic, K. Lee, and S. M. Lukic, "Multifrequency inductive power transfer," *IEEE Trans. Power Electron.*, vol. 29, no. 11, pp. 5995–6005, 2014.

[7] V. G. Agelidis and D. Vincenti, "Optimum non-deterministic pulse-width modulation for three-phase inverters," in *Proceedings Int. Conf. Industrial Electronics, Control, and Instrumentation (IECON '93)*, Nov 1993, pp. 1234–1239 vol.2.

[8] S. Brueske, G. De Carne, and M. Liserre, "Multi-frequency power transfer in a smart transformer based distribution grid," in *40th Ann. Conf. IEEE Industrial Electronics Society (IECON 2014)*, Dallas, US, Oct. 2014, pp. 4325–4331.

[9] S. Brueske, G. Buticchi, and M. Liserre, "Control strategies for multi-frequency power transfer in a smart-transformer-fed low-voltage grid," presented at the 13th IEEE Int. Conf. Industrial Informatics (INDIN 2015), Cambridge, UK, 2015.

[10] M. L. Gasperi, "Life prediction modeling of bus capacitors in AC variable-frequency drives," *IEEE Trans. Ind. Appl.*, vol. 41, no. 6, pp. 1430–1435, Nov 2005.

[11] Y. Weens, N. Idir, R. Bausiere, and J. J. Franchaud, "Modeling and simulation of unshielded and shielded energy cables in frequency and time domains," *IEEE Trans. Magn.*, vol. 42, no. 7, pp. 1876–1882, July 2006.

[12] K. Steinbrich, "Untersuchungen zum frequenzabhängigen Übertragungsverhalten von Enegiekabeln," Ph.D. dissertation, Universität Duisburg-Essen, 2005.

[13] J. Arrillaga and N. R. Watson, "Effects of harmonic distortion," in *Power System Harmonics*. Wiley, 2004, pp. 143–189.